

## Asymmetry in Colloidal Diffusion near a Rigid Wall

Mauricio D. Carbajal-Tinoco,<sup>1</sup> Ricardo Lopez-Fernandez,<sup>1</sup> and José Luis Arauz-Lara<sup>1,2</sup>

<sup>1</sup>*Departamento de Física, Cinvestav, Avenida IPN 2508, Colonia Zacatenco, 07360 México D.F., Mexico*

<sup>2</sup>*Instituto de Física “Manuel Sandoval Vallarta,” Universidad Autónoma de San Luis Potosí,*

*Alvaro Obregón 64, 78000 San Luis Potosí, S.L.P., Mexico*

(Received 18 May 2007; published 28 September 2007)

The three-dimensional motion of single colloidal particles close to a plane wall is measured by optical microscopy. In accordance with classical theoretical predictions, we find an asymmetric motion of the particles in the directions parallel and perpendicular to the wall. We also find that, close to the wall, the distribution functions of perpendicular steps are asymmetric, being shorter toward the wall and longer away from it.

DOI: [10.1103/PhysRevLett.99.138303](https://doi.org/10.1103/PhysRevLett.99.138303)

PACS numbers: 82.70.Dd, 05.40.-a, 47.60.+i, 83.50.Ha

A classical problem in colloidal physics is the description of the motion of single colloidal particles near a flat wall. In the absence of particle-wall direct interactions, other than excluded volume, one is concerned here with the treatment of their complex hydrodynamic interactions. Calculations of the one-body friction, based on linearized creeping flow hydrodynamics, have been carried out predicting dramatic changes in that quantity, namely, close to a wall the friction becomes a tensor whose components increase monotonically as the particle-wall distance  $h$  decreases [1,2]. Verification of such predictions has been a challenge to experimentalists for more than four decades. Besides its scientific importance, such asymmetry makes colloidal motion a highly sensitive probe of the presence of boundaries, both in distance and orientation. Hence, its accurate description and measurement could be of great importance in various fields of science and technology to probe the structure (and dynamics) of complex environments.

In the bulk, the particles' mean squared displacement (MSD)  $\langle \Delta r^2(t) \rangle$  obeys the scalar equation  $\langle \Delta r^2(t) \rangle = 6D_0t$ , where  $D_0$  is the free-diffusion constant, a scalar quantity determined by the fluid and particle properties through the Stokes-Einstein relation (namely,  $D_0 = kT/3\pi\eta\sigma$ , with  $kT$  being the thermal energy,  $\eta$  the bulk shear viscosity of the fluid, and  $\sigma$  the particle's hydrodynamic diameter). Close to a wall, the MSD is split in the motion parallel [along the plane ( $x, y$ )] and perpendicular (along the direction  $z$ ) to the wall, with both quantities depending on  $h$ :

$$\langle \Delta x_h^2(t) \rangle = \langle \Delta y_h^2(t) \rangle = 2D_{\parallel}(h)t, \quad (1)$$

$$\langle \Delta z_h^2(t) \rangle = 2D_{\perp}(h)t, \quad (2)$$

where  $\Delta x_h(t)$  is the displacement along the direction  $x$  during the time  $t$ , of a particle positioned at a distance  $h$  from the wall at  $t = 0$ . The angular parentheses represent an equilibrium ensemble average. Similar definitions follow for the displacements along the directions  $y$  and  $z$ . The quantities  $D_{\parallel}(h)$  and  $D_{\perp}(h)$  are the diffusion coefficients

corresponding to the motion of the particle along the directions parallel and perpendicular to the wall, respectively. The theoretical functional forms for both coefficients are provided in the literature, and are reproduced below when they are used in comparison with the experimental results of this work. In addition to the asymmetry in the parallel and perpendicular directions, the analysis of the perpendicular motion reveals an asymmetric distribution of steps along the  $z$  direction when the particle moves close to the wall; i.e., the distribution functions of perpendicular displacements  $P_h(\Delta z, t)$  deviate from the Gaussian form, being shorter toward the wall and longer away from it.

Experimental studies of the diffusion of colloidal particles close to a rigid wall, performed using evanescent wave dynamic light scattering (introduced in Ref. [3] in the context of polymer physics), have reported an increasing hindering of the particles diffusion as they are closer to the wall [4,5], and an asymmetry between the parallel and perpendicular diffusion modes [6]. Total internal reflection fluorescence microscopy has also been used to measure both modes, finding agreement with the theoretical predictions for the parallel mode but discrepancies for the perpendicular mode [7]. Both techniques measure the dynamics of the particles close to the surface of the wall within a range of distances determined by the penetration depth of the evanescent wave (on the order of the wavelength of the illuminating light). On the other hand, the perpendicular and parallel diffusion of colloidal particles confined between two plates have been measured by optical video microscopy [8]. In such experiments, the  $z$  coordinate is inferred from the particle's diffraction pattern by comparing it with a calibration set of images. That method allows tracking of three-dimensional (3D) excursions, but it is restricted to short trajectories of extension comparable to the particle's diameter.

We present here a direct measurement of the diffusion motion of a single colloidal particle near a rigid wall. Figure 1 shows a scheme of the system. We have implemented an optical microscopy method that allows us to track the actual 3D particle's trajectory in a wide range of

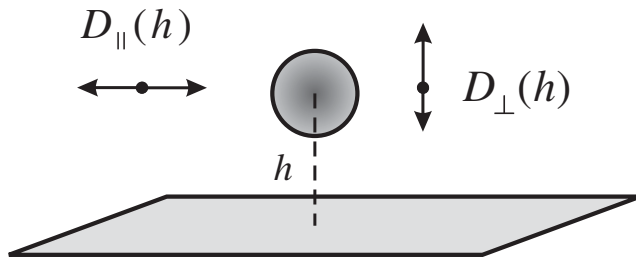


FIG. 1. Scheme of the system: a colloidal particle moving near a rigid plane, with  $h$  being the particle-wall separation. The diffusion of the particle parallel to the wall  $D_{\parallel}(h)$  differs from that perpendicular to the wall  $D_{\perp}(h)$ . There is also an asymmetry in the perpendicular steps.

the  $(x, y, z)$  space. From the trajectory we determine, directly and independently, the mean squared displacements along the three spatial directions as functions of  $h$ . The system studied here consists of highly dilute suspensions of fluorescent polystyrene spheres of diameter  $\sigma = 1.01 \mu\text{m}$ , with 3% of size polydispersity. The suspending fluid is distilled deionized water at 10 mM of NaCl. The suspension is loaded in a glass cell consisting of a slide and a cover slip separated by spacers of thickness  $300 \mu\text{m}$ . The sample is placed on the stage of an optical fluorescence microscope, equipped with a digital charge coupled device (CCD) and a piezo nanofocussing device with nanometer vertical resolution. The sample is allowed to equilibrate at room temperature for 3 h. During this time, particles settle close to the bottom surface due to gravity but they remain in constant Brownian motion. The added electrolyte provides a screening length of  $5 \pm 2 \text{ nm}$ . In order to avoid any influence of both the van der Waals and the electrostatic interactions between the particles and the glass surface, in this work we only consider the motion of particles whose surface is away from the wall distances several times the screening length. Therefore, in our experiments the only interactions between a particle and the wall are hydrodynamic. We observed sites in the sample where only two particles were within the field of view of  $150 \times 150 \mu\text{m}^2$ . One of the particles was moving close to the wall while the second particle was fixed to it (by van der Waals forces) and it is used as a reference to locate the surface of the wall. In all cases, both particles were separated more than  $30 \mu\text{m}$ , avoiding in this way any influence of the fixed particle on the motion of the mobile one.

The tracking of the particles' 3D trajectories is done as follows. The sample is observed from a top view using fluorescence illumination. A particle in the focal plane of the microscope optics appears as a bright circular object against a dark background. However, when the particle is out of focus, the optics detects a cross section of the point spread function (PSF) of the particle [9,10]. The image at the focal plane of a particle out of focus in the direction away from the microscope objective consists of concentric rings whose number and diameter increase monotonically

with its distance from the focal plane. Figure 2 shows images of the pattern observed when the particle is at distances of  $8.6 \mu\text{m}$  [Fig. 2(a)] and  $6.9 \mu\text{m}$  [Fig. 2(b)] from the focal plane, away from the microscope objective. As one can see here, the diameter of the more external ring is larger for particles further away from the focal plane. Figure 2(c) shows the experimental determination of the (monotonic) correspondence curve between the radius  $R$  of the external ring and the distance  $\Delta z$  of the particles' center from the focal plane. Such a curve is determined by taking images of a fixed particle at the bottom surface and moving the focal plane of the objective upward using the piezoelectric device attached to it. Thus, a set of images of known  $\Delta z$  are obtained, and the corresponding value of  $R$  is determined in each of them as follows. The position  $(x, y)$  of the center of the pattern is determined using a standard procedure [11]. Then, the average profile of light intensity  $I(r)$  is measured in each image as a function of the radial distance  $r$  from the center of the pattern; i.e., we average the light intensity along a ring [centered at  $(x, y)$ ] of radius  $r$  and 1 pixel width. The inset in Fig. 2(c) shows a typical profile  $I(r)$  consisting of local maxima and minima, in correspondence with the rings. As one can see here, the external ring shows a well-defined maximum whose position  $R$  can be located quite accurately. In Fig. 2(c) we plot two sets of measurements of  $R$  vs  $\Delta z$  (symbols), showing the reproducibility of the relation. The solid line is an exponential function, which is the best fit to both sets of experimental data. Thus, given the monotonic relation between  $R$  and  $\Delta z$ , we can use the former as a direct measurement of the  $z$  coordinate of the particle (with

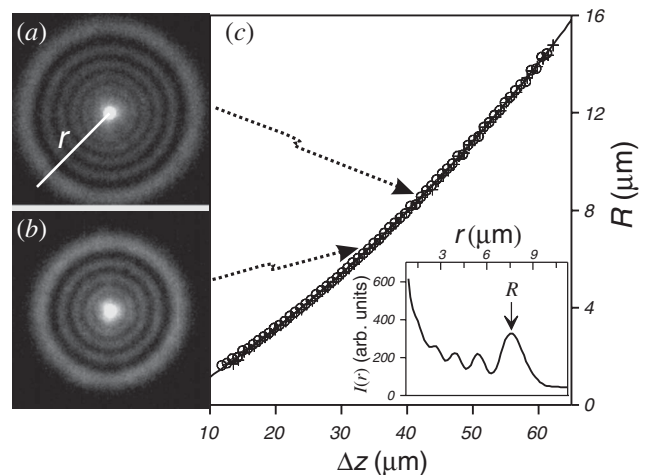


FIG. 2. Images of the cross section of the PSF of a  $1.01 \mu\text{m}$  fluorescent particle out of focus  $8.6 \mu\text{m}$  (a) and  $6.9 \mu\text{m}$  (b), in the direction away from the microscope objective. The relation between the radius  $R$  of the external ring of the PSF and the distance of the particle to the focal plane  $\Delta z$  is shown in (c), the symbols represent two sets of experimental data and the solid line a fit to an exponential function. The inset in (c) shows a typical profile of the light intensity.

respect to the focal plane). Thus, the 3D trajectory of a single mobile particle is obtained by analyzing consecutive frames, with a time interval  $\Delta t = 33.33$  ms, to determine the three spatial coordinates in each of them as described here.

As we explained above, we locate sites in the sample with only two particles in the field of view, one moving close to the bottom surface and the other fixed to it (the reference to determine  $h$ ). The motion of the mobile particle is recorded in series of 2000 consecutive frames which are analyzed to obtain the particle's 3D trajectory. During one run of  $2000\Delta t$ , the trajectory extends over several times  $\sigma$  along  $z$ , sampling in this way a wide range of the distance  $h$ . In order to determine the dependence on  $h$  of the diffusion coefficients, we define discrete values of  $h$  with a width of  $\sigma/2$ . Then, we divide the trajectory in short traces of  $N$  consecutive time steps. The initial position  $z$  of each short trace will fall within one of the discrete values of  $h$ . From the short trajectories we determine the MSDs along  $x$ ,  $y$ , and  $z$ , pertaining to each value of  $h$ . The diffusion coefficients are then obtained as the initial slope of the corresponding MSD as indicated by Eqs. (1) and (2). The results shown below are the average of data from several ( $\sim 200$ ) different trajectories of 2000 time steps each, observed both at different sites on the same sample and in different samples, to ensure reproducibility and to avoid bias from sample preparation. All the results reported here correspond to the analysis of the trajectories divided in segments of  $N = 5$  time steps, but other values of  $N$  within the range of 3 to 7 lead to similar results.

Figure 3 shows the results obtained for the normalized diffusion coefficient parallel to the wall (symbols) as a function of the particle-wall separation  $h$ . The normalizing

quantity  $D_S$  is the average value of the self-diffusion coefficient of different isolated particles, measured far away from the wall where the diffusion is isotropic and independent of  $h$ .  $D_S$  is found to be very close (within 2%) of the theoretical value  $D_0$  calculated using the nominal diameter. As one can see here, the effect of the particle-wall hydrodynamic interactions on the particles' parallel motion leads to a significant reduction of  $D_{\parallel}(h)$  as the particle approaches the wall. The effect is of long range, spanning over more than 20 particles' diameters where  $D_{\parallel}(h)$  slowly approaches its asymptotic value  $D_S$ . In Fig. 3 we compare our experimental data with the predictions of Eq. (3) (dashed line), taken from Ref. [2], given as

$$\frac{D_0}{D_{\parallel}(h)} = 1 - \frac{8}{15} \ln(1 - \beta) + 0.029\beta + 0.04973\beta^2 - 0.1249\beta^3 + \dots, \quad (3)$$

where  $\beta = \sigma/2h$ . As one can see here, there is an excellent agreement between experiment and theory over a wide range of particle-wall separations. As a manner to illustrate the capabilities of the method employed here, in the inset of Fig. 3 we show the 3D trajectory of a particle diffusing close to the wall. As one can see here, the effect of gravity is only evident at long times ( $\sim 1000\Delta t$ ), but not at the short-time scale of few time steps where we determine the diffusion coefficients.

Figure 4 shows the experimental results (solid circles) for the diffusion coefficient corresponding to the perpendicular motion. As one can see here, the hindering of the perpendicular motion as the particle approaches the wall is more pronounced than that for the parallel motion, which is in agreement with the theoretical results of Eq. (4) (dashed

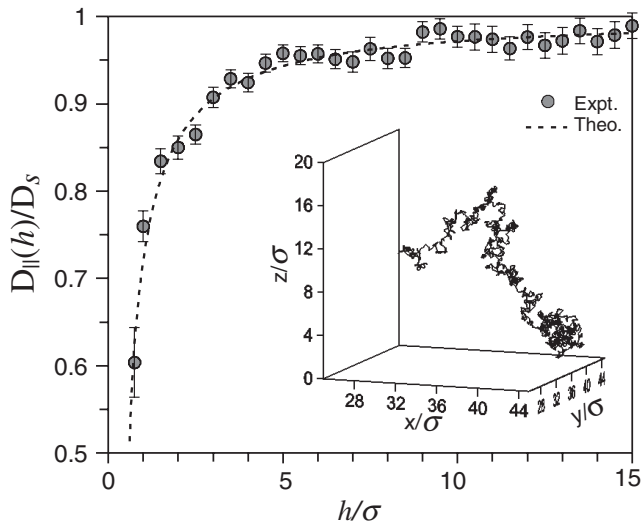


FIG. 3. Diffusion coefficient for the motion parallel to the wall as a function of  $h$ , experiment (symbols) and theory (dashed line). The inset shows the 3D trajectory of a particle diffusing near the wall, located at  $z = 0$ .

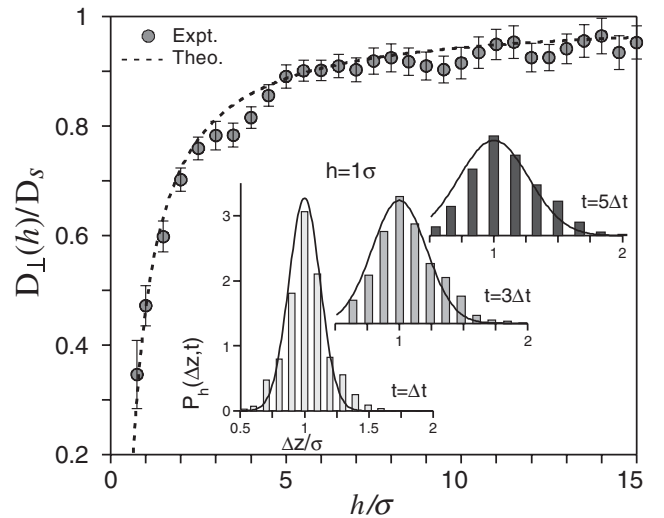


FIG. 4. Diffusion coefficient for the perpendicular motion (solid circles). The dashed line represents the prediction of Eq. (4). The inset shows  $P_h(\Delta z, t)$  (bars), for 3 times, measured at  $h = 1\sigma$ . Solid lines represent Gaussian functions of width  $2D_{\perp}(h)t$ ; see text.

line), taken from Ref. [1], given as

$$\frac{D_0}{D_{\perp}(h)} = \frac{4}{3} \sinh\alpha \sum_{n=1}^{\infty} \frac{n(n+1)}{(2n-1)(2n+3)} \times \left[ \frac{2 \sinh(2n+1)\alpha + (2n+1) \sinh 2\alpha}{4 \sinh^2(n+\frac{1}{2})\alpha - (2n+1)^2 \sinh^2\alpha} - 1 \right], \quad (4)$$

where  $\alpha = \cosh^{-1}(2h/\sigma)$ .

From the 3D trajectories one can determine other, more fundamental quantities, describing single particle dynamics, namely, the density probability distribution functions of particles' steps  $P_h(\Delta x, t)$ ,  $P_h(\Delta y, t)$  and  $P_h(\Delta z, t)$ , where  $P_h(\Delta x, t)dx$  is the probability that a displacement along the direction  $x$  during the time  $t$ , of a particle located at  $z = h$  at time  $t = 0$ , falls around the value  $\Delta x$  within a width  $dx$  (similar definitions follow for distributions along  $y$  and  $z$ ). In the bulk, these distribution functions are Gaussian functions of width  $2D_S t$ . However, close to a wall these functions depend on the direction of motion and also on the particles separation to the wall. In our system, the distribution functions along  $x$  and  $y$  are indeed symmetric and follow Gaussian functions of width  $2D_{\parallel}(h)t$  (data not shown). In contrast, the distributions along  $z$  are not symmetrically distributed around  $\Delta z_h(t) = 0$ . The inset in Fig. 4 shows  $P_h(\Delta z, t)$ , measured at  $h = \sigma$  (bars), for 3 different times within the interval used to determine the diffusion coefficients. Here one can see clearly the asymmetry in the step distribution functions, being shorter in the direction toward the wall and longer in the direction away from it. One can also see that such asymmetry increases with time. For comparison, we present in solid lines the corresponding Gaussian functions  $[1/4\pi D_{\perp}(h)t]^{(1/2)} \times \exp[(\Delta z - h)^2/4D_{\perp}(h)t]$  where  $D_{\perp}(h)$  is calculated using Eq. (4). In order to rule out any effect from gravity in this asymmetry, measurements were also carried out on particles diffusing close to the top surface of the sample cell using an inverted microscope. Similar results are obtained from both setups, and in Fig. 4 the results presented are the average of both measurements. Let us note here, that each one of the histograms in Fig. 4 was constructed from  $\sim 1500$  measured values of  $\Delta z_h$ .

An asymmetry in the distribution of steps is predicted for one-dimensional random walks in the presence of a reflecting barrier, which reflects back the long trajectories in the direction toward it [12]. In such case  $\langle \Delta z(t) \rangle$  increases with time, provided the time is long enough that the particle can reach the barrier. In the inset of Fig. 4 we show the results for the distribution functions measured at  $h = 1\sigma$ . There, one can see that  $\Delta z$  toward the wall is indeed impeded to reach values larger than its maximum approaching distance  $h - \sigma/2$ . Thus, the predictions of the

reflecting barrier model seem to be applicable to this case. However, in our system we measure  $P_h(\Delta z, t)$  in a wide range of values of  $h$  and the asymmetry is observed for values of  $h$  up to  $7\sigma$ , although it becomes less pronounced as  $h$  increases. As explained above, at each value of  $h$  we consider only the local diffusion (i.e., short-time scale), such that the particles' excursions along all directions are smaller than the particles' size. Thus, for  $h \geq 2\sigma$  the asymmetry can not be solely the result of the reflected trajectories at the wall, but it also contains the effect of the long-range hydrodynamic interactions which contribute to the hindering (reflection) of long excursions toward the wall, even when the particles are not close to contact.

In this work we address a classical problem in colloidal hydrodynamics, namely, the effect of the hydrodynamic interactions on the motion of single colloidal particles near a rigid plane wall. Our results confirm the long-standing theoretical predictions of the asymmetry between the parallel and perpendicular motions. We also report an asymmetry in the distribution of perpendicular steps, due to the particles' trajectories reflection by the wall, an effect found here to be enhanced by the particle-wall hydrodynamic interactions.

The authors acknowledge technical support from D. Jacinto, and financial support from Consejo Nacional de Ciencia y Tecnología, México, Grant No. 49486 and No. 46121.

- 
- [1] J. Happel and H. Brenner, *Low Reynolds Number Hydrodynamics* (Kluwer Academic Publishers Group, Dordrecht, The Netherlands, 1983).
  - [2] G. S. Perkins and R. B. Jones, *Physica* (Amsterdam) **189A**, 447 (1992).
  - [3] J. Gao, K. F. Freed, and S. A. Rice, *J. Chem. Phys.* **93**, 2785 (1990); B. Lin, S. A. Rice, and D. A. Weitz, *J. Chem. Phys.* **99**, 8308 (1993).
  - [4] N. Garnier and N. Ostrowsky, *J. Phys. II* (France) **1**, 1221 (1991).
  - [5] R. J. Oetama and J. Y. Walz, *J. Chem. Phys.* **124**, 164713 (2006).
  - [6] P. Holmqvist, J. K. G. Dhont, and P. R. Lang, *Phys. Rev. E* **74**, 021402 (2006).
  - [7] A. Banerjee and K. D. Kihm, *Phys. Rev. E* **72**, 042101 (2005).
  - [8] B. Lin, J. Yu, and S. A. Rice, *Phys. Rev. E* **62**, 3909 (2000).
  - [9] S. Frisken Gibson and F. Lanni, *J. Opt. Soc. Am. A* **8**, 1601 (1991).
  - [10] J. S. Park, C. K. Choi, and K. D. Kihm, *Meas. Sci. Technol.* **16**, 1418 (2005).
  - [11] J. Santana-Solano, A. Ramírez-Saito, and J. L. Arauz-Lara, *Phys. Rev. Lett.* **95**, 198301 (2005).
  - [12] S. Chandrasekhar, *Rev. Mod. Phys.* **15**, 1 (1943).